Electrochemical Impedance Spectroscopy Study of a Hydrogen Electrode Reaction at a Zn Electrode in a Molten LiCl−KCl−LiH System

Hironori Nakajima, Toshiyuki Nohira,* and Yasuhiko Ito*

Department of Fundamental Energy Science, Graduate School of Energy Science, Kyoto University, Sakyo-ku, Kyoto 606-8501, Japan

Received: December 5, 2004; In Final Form: March 17, 2005

The hydrogen electrode reaction involving hydride ion, H^-, at a Zn electrode is investigated in a molten LiCl−KCl−LiH system at 673 K. The charge-transfer resistances were measured by electrochemical impedance spectroscopy in the overpotential region of $0.10 \leq \eta \leq 0.35$ V and over the H^- concentrations of $1.5 \times 10^{-4} \leq C_{H^-} \leq 1.2 \times 10^{-3}$ mol cm^{-3}. The logarithm plot of the charge-transfer resistance against the overpotential at $C_{H^-} = 3.0 \times 10^{-4}$ mol cm^{-3} gives the symmetry factor, β, of 0.50 and the exchange current density, j_0, of 5.8×10^{-3}A cm^{-2}, respectively. Analysis of the dependence of j_0 on H^- concentration independently gives a β of 0.55. The reasonable β values indicate that the $H^- \rightleftharpoons H_{ad}(M) + e^-$ step is rate-determining.

Introduction

Hydride ions (H^-) have been reported to exist in molten alkali metal halides containing alkali metal hydrides, such as a molten LiCl−KCl−LiH system.[1,2] The hydrogen electrode reaction involving H^- ion in a molten LiCl−KCl−LiH system is worth studying from both engineering and scientific aspects. From an engineering point of view, there are several promising applications that use electrochemical reactions involving H^- ions, for example, the Li−H_2 thermally regenerative fuel cell,[1,3,4] tritium recovery from molten salt for a thorium molten salt reactor and fusion reactor,[5−7] an SiH_4 production in molten alkali halides for the industrial manufacture of Si semiconductors.[8] The electrochemical reaction of the H^- ion also provides a precise and convenient means to investigate both thermodynamic and kinetic behaviors of metal-hydride systems at high temperatures.[9−11] Related with these applications, there have been a number of studies that deal with the anodic[2,12−14] and cathodic[15−17] hydrogen electrode reaction in molten LiCl−KCl−LiH systems. However, kinetic parameters such as the exchange current density and symmetry factor have not been evaluated so far. The kinetic parameters directly represent the electrocatalytic activity of electrode materials, which are of great use for engineering applications in accelerating the reaction and reducing overpotentials.

From a scientific point of view, the elucidation of the mechanism of the hydrogen electrode reaction involving the H^- ion is of great interest as well. In aqueous solution systems, a number of kinetic investigations have been carried out on the hydrogen electrode reaction involving the H^+ (H_3O^+) ion or H_2O, and the relation between the reaction mechanism and electrocatalytic activity has been revealed. It has been reported that the characteristics of the electrode materials such as the electronic work function, the adsorption enthalpy of the hydrogen atom, and the electron state are related to the electrocatalytic activity.[18−20] These studies have explained differences in the exchange current density among the electrode materials; for example, the exchange current density for Pd is about 10^{10} times larger than that for Pb. It seems quite interesting to compare the kinetic parameters and reaction mechanism in molten LiCl−KCl−LiH systems with those in the aqueous systems, which might contribute to further develop the theories for both systems. Our preliminary experiments on Zn, Ti, Ni, and Pd electrodes using electrochemical impedance spectroscopy (EIS) have revealed that the charge-transfer resistances for Ni and Pd are very small while those for Zn and Ti are not so small.[21] This catalytic effect is similar to that for the hydrogen electrode reaction in the aqueous systems. In the aqueous systems, the adsorbed hydrogen atom has been reported to play a significant role for the catalytic effect.[18−20] Thus, the above catalytic effect in a molten LiCl−KCl−LiH system is possibly due to adsorbed hydrogen atoms as well.

From such a background, we have begun the kinetic studies on the hydrogen electrode reactions in a molten LiCl−KCl−LiH system. As a starting point, Zn is selected since it is difficult to precisely evaluate small charge-transfer resistances for metals such as Ni and Pd without a special measuring method with a higher time resolution. For Ti, a more complicated treatment would be necessary because of its large hydrogen absorption property. In this paper, the kinetic parameters for a Zn electrode are evaluated by the EIS measurements, and the reaction mechanism is discussed.

Theoretical Section

The hydrogen electrode reaction involving the H^- ion possibly proceeds by two different paths in the anodic direction. One is

$$H^- \rightleftharpoons H_{ad}(M) + e^- \quad \text{(A)}$$

followed by

$$2H_{ad}(M) \rightleftharpoons H_2 \quad \text{(B)}$$

and the other is the reaction A followed by

$$H_{ad}(M) + H^- \rightleftharpoons H_2 + e^- \quad \text{(C)}$$

* Authors to whom correspondence should be addressed. E-mail: nohira@energy.kyoto-u.ac.jp; y-ito@energy.kyoto-u.ac.jp.

10.1021/jp044477z CCC: $30.25
Published on Web 04/13/2005

The A−B scheme, i.e., a charge-transfer reaction is followed by a recombination reaction, is analogous to the Volmer−Tafel reaction in the aqueous systems, while the A−C scheme, i.e., a charge-transfer reaction is followed by another charge-transfer reaction, is analogous to the Volmer−Horiuti (or Volmer−Heyrovsky) reaction.[22,23] In analogy with the theory of the Volmer reaction, the current density associated with the charge-transfer reaction A is written as[22]

$$j = j_0\left\{\frac{1-\theta}{1-\theta_0}\exp\left(\frac{\beta F}{RT}\eta\right) - \frac{\theta}{\theta_0}\exp\left[-\frac{(1-\beta)F}{RT}\eta\right]\right\} \quad (1)$$

where j_0 is the exchange current density and θ and θ_0 are the degrees of coverage of hydrogen atoms at the nonequilibrium and equilibrium states, respectively. Here, β is the symmetry factor, and η is the overpotential. The other variables (F, R, and T) have their common meanings. Thus, the charge-transfer resistance, r_{ct}, is expressed as

$$r_{ct} = \left(\frac{\partial\eta}{\partial j}\right)_\theta = \frac{RT}{Fj_0}\left\{\frac{1-\theta}{1-\theta_0}\beta\exp\left(\frac{\beta F\eta}{RT}\right) + \frac{\theta}{\theta_0}(1-\beta)\exp\left[-\frac{(1-\beta)F\eta}{RT}\right]\right\}^{-1} \quad (2)$$

Assuming $(1-\theta)/(1-\theta_0) \approx 1$ in the measured potential region and η is large enough to neglect the backward reaction, eq 2 yields

$$r_{ct} = \frac{RT}{\beta F j_0}\exp\left(-\frac{\beta F\eta}{RT}\right) \quad (3)$$

Here, r_{ct} is measured by a method having high time resolution such as the EIS method with a high frequency. Finally, the following equation is derived.

$$\ln r_{ct} = \ln\frac{RT}{\beta F j_0} - \frac{\beta F}{RT}\eta \quad (4)$$

If reaction A is the rate-determining process, β is obtained from the gradient of the $\ln r_{ct}-\eta$ plot, and j_0 can be obtained by extrapolating the plot to $\eta = 0$ according to above equation.

The symmetry factor is also accessible from the dependence of j_0 on the concentration of the H^- ion in the bulk, C_{H^-}, as follows. The exchange current density for reaction A is expressed as where k^0 is the standard rate constant and E and

$$j_0 = Fk^0(1-\theta_0)C_{H^-}\exp\left[\frac{-\beta F}{RT}(E - E_m^{0'})\right] \quad (5)$$

$E_m^{0'}$ are the equilibrium potential and the standard formal potential, respectively. The relation between E and $E_m^{0'}$ is expressed as the following Nernst equation.

$$E = E_m^{0'} + \frac{RT}{F}\ln\frac{(P_{H_2}/P_{H_2}^0)^{1/2}}{C_{H^-}/C_{H^-}^0} \quad (6)$$

The standard pressure and standard concentration are defined as $P_{H_2}^0 = 1$ atm and $C_{H^-}^0 = 1$ mol cm^{-3}, respectively. Substitution of eq 6 in eq 5 and taking the logarithm result in

$$\ln j_0 = \ln\{Fk^0(1-\theta_0)\} + (1-\beta)\ln C_{H^-} + \beta\ln(P_{H_2}/P_{H_2}^0)^{1/2} + \beta\ln C_{H^-}^0 \quad (7)$$

Since θ_0 should be independent of C_{H^-}, differentiating eq 7 with respect to $\ln C_{H^-}$ at a constant P_{H_2} gives

$$\left(\frac{\partial\ln j_0}{\partial\ln C_{H^-}}\right)_{P_{H_2}} = 1-\beta \quad (8)$$

Hence, eq 8, which corresponds to the reaction order, gives β.

Experimental Section

The experiments were carried out in an argon glovebox with a gas circulating purifier (MIWA MFG Co., Ltd.). All chemicals were anhydrous reagent grade. A eutectic mixture of LiCl (99.0%, Wako Pure Chemical Industries, Ltd.) and KCl (99.5%, Wako Pure Chemical Industries, Ltd.) was prepared (LiCl/KCl = 0.585/0.415, in mole fraction) in a high-purity alumina crucible (Nikkato Co., Ltd., SSA-S, 99.5% Al_2O_3) and dried in a furnace under vacuum at 473 K for at least 24 h. After that, it was melted at 673 K. To remove residual water and metal impurities, pre-electrolysis was carried out using a Ni plate cathode with a glassy carbon anode until the residual cathodic current density became less than 0.3 mA cm^{-2}. LiH (97.0+ wt %, Wako Pure Chemical Industries, Ltd.) was added into the melt as a H^- ion source. The anion fraction of the H^- ion was confirmed in situ by comparing the anodic peak current density obtained by cyclic voltammetry with a calibration curve, then converted to a molar density expression. The calibration curve was prepared beforehand considering the small amount of LiH consumed by residual contaminations in the melt in the same manner reported previously.[14] A chromel−alumel thermocouple was used for the temperature measurement.

A schematic drawing of the experimental apparatus is shown in Figure 1. The working electrode was a Zn plate (99.99%, ϕ 6 mm × 0.2 mm, Nilaco Co.), which was fully immersed in the molten salt. A Mo plate (99.95%, ϕ 6 mm × 0.2 mm, Nilaco Co.) was also used as the working electrode for linear sweep voltammetry. The Zn plate was polished with an emery paper, and the Mo plate was electrochemically polished in sulfuric acid pretreatments. The counter electrode was an Al−Li alloy prepared by electrolytic deposition of Li on an Al plate (99.5%, 10 mm × 40 mm × 2 mm, Nilaco Co.). The reference electrode was an Al−Li alloy in the coexisting ($\alpha + \beta$) phase state prepared electrochemically from an Al wire (99.99%, 5 mm × ϕ 1 mm, Nilaco Co.). The following reversible reaction determines the equilibrium potential of this electrode.[24−26]

$$Al(\alpha) + Li^+ + e^- \rightleftharpoons AlLi(\beta) \quad (9)$$

The potential of this reference electrode was calibrated with reference to that of the Li^+/Li electrode, which was prepared by electrodepositing lithium metal on a nickel wire.

Linear sweep voltammetry was performed with a potentiostat (Solartron 1287) controlled by a personal computer. The EIS measurement was performed with a frequency response analyzer (Solartron 1260) connected with a potentiostat (Solartron 1287) controlled by a personal computer. The frequency range was 0.1 Hz to 50 kHz. The amplitude of the sinusoidal potential was 5 mV. The electrode potential was always varied from positive to negative to avoid the formation of Zn−Li alloy[27] both in linear sweep voltammetry and in the EIS measurement. The overpotential was determined from the deviation of applied potential from the H_2/H^- equilibrium potential. The H_2/H^- equilibrium potential at $P_{H_2} = 1$ atm and $T = 673$ K was obtained from the Nernst equation, in which the standard formal potential is calculated to be 0.055 V (vs Li^+/Li) from our earlier thermodynamic study.[28] In addition, our previous thermody-

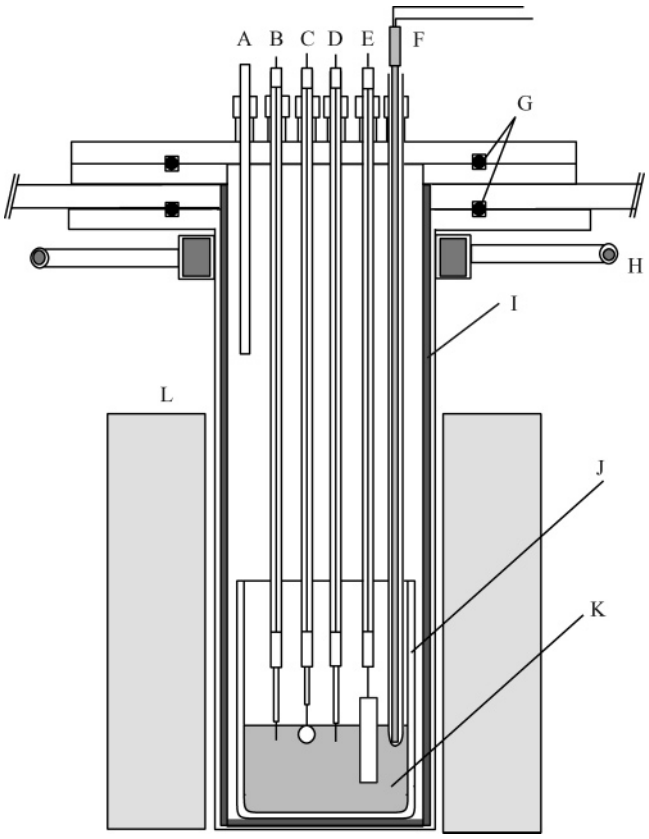

Figure 1. Schematic drawing of the experimental apparatus. (A) Ar and H_2 gas inlet and outlet; (B) dynamic reference electrode; (C) working electrode; (D) reference electrode; (E) counter electrode; (F) thermocouple; (G) O-ring; (H) water cooling pipe; (I) stainless holder; (J) alumina crucible; (K) molten LiCl−KCl−LiH; (L) heater.

TABLE 1: Estimated Solubilities of LiH in a Molten LiCl−KCl System

temperature/K	ΔG_f^0(crystal)/ kJ mol^{-1}	solubility/ 10^{-3} mol cm^{-3}	solubility/anion fraction
673	−37.904	2.5	0.084
723	−33.684	4.4	0.13
773	−29.500	6.5	0.18
823	−26.106	8.3	0.22
873	−21.240	14	0.32

namic study gives the solubility of LiH by the following calculation. Since the chemical potential of dissolved LiH in the melt is equal to that of the crystal LiH at the saturation concentration, the solubility of LiH can be estimated by introducing the standard free energy change of formation of crystalline LiH, ΔG_f^0(crystal), divided by F into the left-hand side of the Nernst equation, eq 6, assuming that the activity coefficient of the H^- ion is constant in the region from dilute concentration to the saturation concentration. Then, the solubilities are estimated for several temperatures using $E_m^{0'}$ and ΔG_f^0(crystal)[29] as shown in Table 1.

Results and Discussion

Linear Sweep Voltammetry. Figure 2 shows linear sweep voltammograms for Zn and Mo electrodes at $C_{H^-} = 2.4 \times 10^{-4}$ mol cm^{-3}. Ohmic drops were compensated using the solution resistances that were obtained from fitting results for impedance plots by using an equivalent circuit in Figure 4 described later. A potential sweep in the negative direction was started from the high-overpotential region to avoid the influence of Zn−Li alloy formation. The cathodic current around $\eta = 0.05$ V is due to Li insertion into the Zn electrode.[27] The limiting current density was 0.10 A cm^{-2}. Figure 3 shows a linear sweep voltammogram at a Zn electrode in a blank system. A very small current was observed in the potential region where the anodic current was observed in Figure 2.

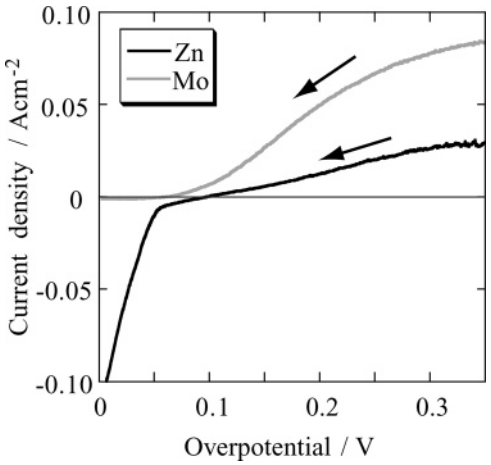

Figure 2. Linear sweep voltammograms for Zn and Mo electrodes in a molten LiCl−KCl−LiH (2.4×10^{-4} mol cm^{-3}) system at 673 K. Scan rate: 5×10^{-3} V s^{-1}.

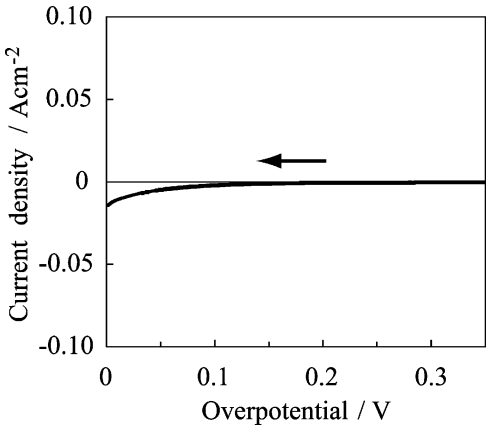

Figure 3. Linear sweep voltammogram for a Zn electrode in a molten LiCl−KCl system at 673 K. Scan rate: 5×10^{-3} V s^{-1}.

The anodic current density for a Zn electrode is apparently smaller than that for a Mo electrode. Since the diffusion of the H^- ion in the melt has been reported to be rate-determining at the Mo electrode,[14] the rate-determining process for a Zn electrode should be different from that for a Mo electrode. The contributions of the A−B scheme or the A−C scheme are likely to play major roles for a Zn electrode. In the present paper, reaction A is, thus, assumed to be the rate-determining process at Zn for evaluating kinetic parameters, of which validity is discussed later.

Electrochemical Impedance Spectroscopy. The EIS measurements were performed in the range $0.10 \le \eta \le 0.35$ V to evaluate the kinetic parameters. C_{H^-} was varied from 1.5×10^{-4} to 1.2×10^{-3} mol cm^{-3}.

Impedance plots were analyzed with an equivalent circuit shown in Figure 4. For a solid electrode, a double-layer capacitance should be substituted with a constant-phase element (CPE) due to the inhomogeneity of the surface.[30] Adsorbed hydrogen atoms are taken into account as a pseudocapacitance (c_{ad}) and a resistance (r_{ad}) with reference to the Armstrong−Henderson equivalent circuit.[31,32] Using this circuit, several researchers have carried out kinetic analyses for the cathodic hydrogen evolution reaction (HER) in aqueous systems,[31−34]

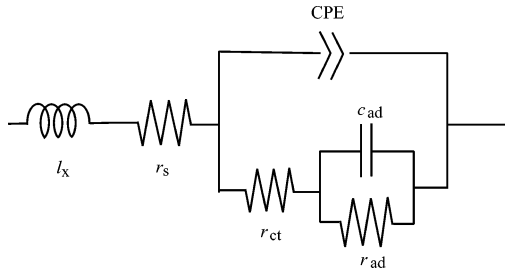

Figure 4. Equivalent circuit: l_x, inductance; r_s, solution resistance; CPE, constant-phase element; r_{ct}, charge-transfer resistance; c_{ad}, pseudocapacitance; r_{ad}, resistance.

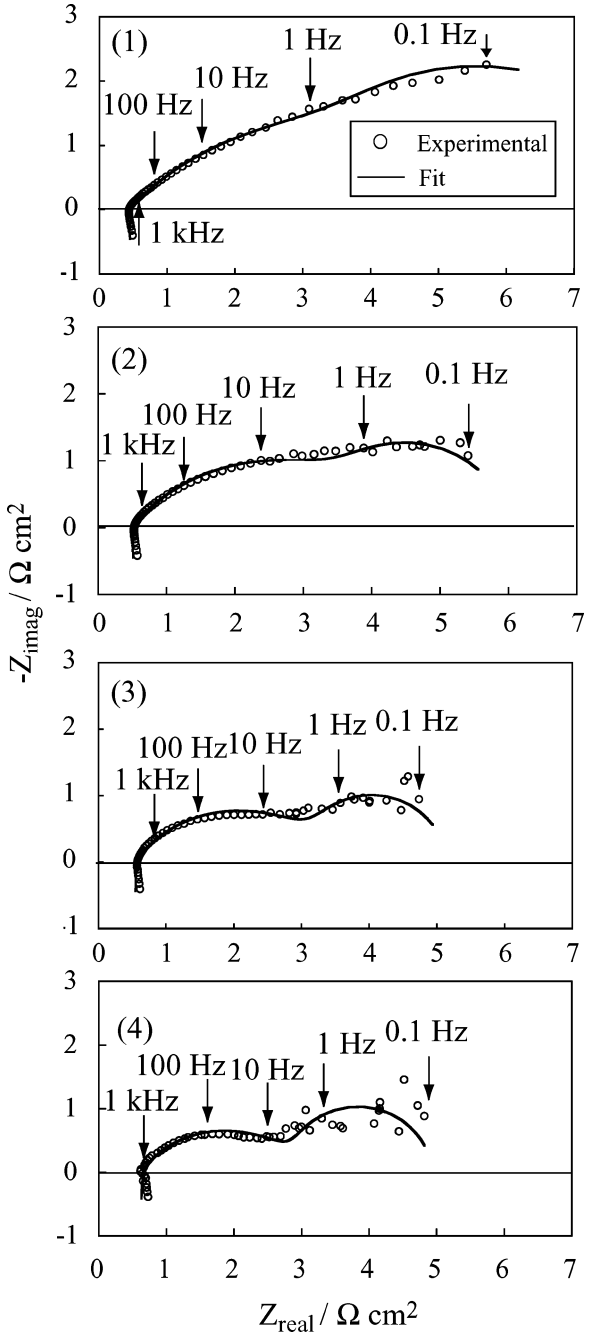

Figure 5. Complex-plane plots for a Zn electrode in a molten LiCl−KCl−LiH (3.0×10^{-4} mol cm^{-3}) system at 673 K: (1) $\eta = 0.16$ V; (2) $\eta = 0.19$ V; (3) $\eta = 0.23$ V; (4) $\eta = 0.27$ V.

which are complementary systems to the present one. An inductance (l_x) is also included in this circuit since inductance was observed in the high-frequency region. This inductance is not ascribed to the lead wire because the measurement for a dummy cell consisting of resistors and condensers with the same lead wire did not yield such inductance. The inductance has been reported in molten salts by Kisza.[35] They explained that the inductance is related to the solvation process of ions. A similar explanation might be possible in the present system. However, since the inductance affects only the plot in the high-frequency region, this does not bring any essential differences in the intended results, i.e., determination of r_{ct}. The Zview program (Scribner Associates Inc.), which is based on the complex nonlinear least-squares (CNLS) technique,[30] was used for the analysis.

Impedance plots (complex-plane plots) at 3.0×10^{-4} mol cm^{-3} are shown in Figure 1 with fitted curves produced by the Zview program. A depressed semicircle is observed in the higher-frequency region for each overpotential. The semicircle is attributed to the charge-transfer resistance. The diameter of the semicircle decreases with increasing overpotential, corresponding to the decrease of the charge-transfer resistance. The plots in the lower-frequency region are fitted with a semicircle ascribed to c_{ad} and r_{ad} although some discrepancies remain, indicating the adsorbed hydrogen atoms. These plots are probably associated with alternating current (ac) perturbation of θ.[31,32] These results are similar to those for the HER at Pt and $MoPt_3$ intermetallic compound in the aqueous systems,[33,34] in which a similar interpretation for the reaction scheme involving the adsorbed hydrogen atoms has been made as that in the present case. This similarity implies that the catalytic effects of the electrodes are similar for both the systems. In the high-overpotential region, the effect of transport is not completely negligible. For instance, at $C_{H^-} = 2.4 \times 10^{-4}$ mol cm^{-3} and $\eta = 0.3$ V, the anodic current density observed is ca. 80% of the charge-transfer current density calculated by the following equation[22]

$$j = j_t\left(1 - \frac{j}{j_l}\right) \tag{10}$$

where j_t and j_l are the charge transfer and the limiting current densities, respectively. However, the ratio is larger at $\eta < 0.3$ V. Hence, the effect of transport is small in the low-overpotential region. The scatterings are explained by the formation and corruption of the adsorbed hydrogen layer or by the changes in the surface area of the electrode due to gas evolution. The effect of convection arising from the gas evolution to the transport of the H^- ion also should be considered in the high-overpotential region. For all H^- concentrations, two semicircles were used for the fit, and the data in the higher-frequency region were used to evaluate r_{ct} values. They have an accuracy between 2 and 11%.

Relations between r_{ct} and η are plotted in Figure 6. These plots are in good agreement with eq 3 in the region of $0.10 \leq \eta \leq 0.25$ V for all cases. In the higher-overpotential region, the deviation of r_{ct} from eq 3 becomes large for each concentration. This may be explained by the deviation from the assumption of $(1 - \theta)/(1 - \theta_0) \approx 1$, whose deviation is due to an increase in θ. That is to say that the increase in θ prevents the decrease of r_{ct}, taking into account eq 2. In the case of $C_{H^-} = 3.0 \times 10^{-4}$ mol cm^{-3}, the following relation is obtained by least-squares fitting for the data at $0.16 \leq \eta \leq 0.25$.

$$\ln r_{ct} = \ln(20) - (8.5)\eta \tag{11}$$

By comparison with eq 4, β and j_0 are calculated to be 0.50 and 5.8×10^{-3} A cm $^{-2}$, respectively. This j_0 value, which is

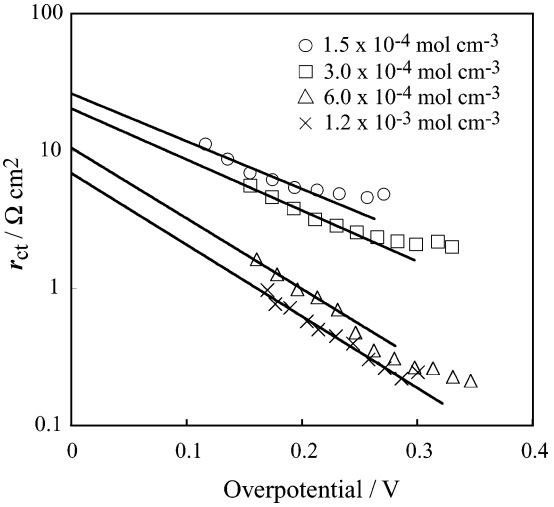

Figure 6. Relation between charge-transfer resistance and overpotential for a Zn electrode at various C_{H^-} values in molten LiCl−KCl−LiH systems at 673 K.

TABLE 2: j_0 and β Values at Different H^- Concentrations[a]

$10^4 \times C_{H^-}$/mol cm^{-3}	$10^3 \times j_0$/A cm^{-2}	β
1.5	4.8	0.46 ± 0.03
3.0	5.8	0.50 ± 0.01
6.0	8.0	0.68 ± 0.02
12	12	0.70 ± 0.01

[a] β values are expressed with the 95% confidence intervals.

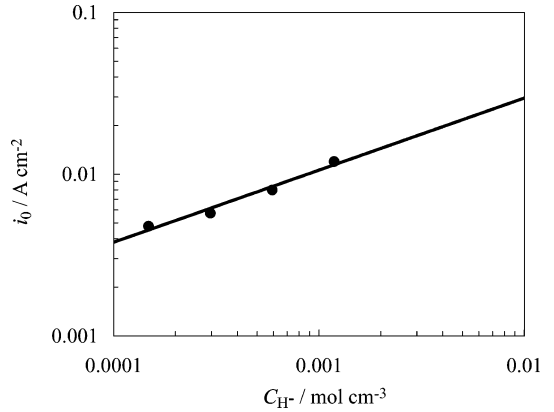

Figure 7. Relation between the exchange current density and the H^- concentration for a Zn electrode in molten LiCl−KCl−LiH systems at 673 K.

on the order of 10^{-3} A cm $^{-2}$, is rather larger than that of the hydrogen electrode reaction at Pt electrodes in the aqueous system at 298 K,[18] which is on the order of 10^{-4} A cm^{-2}. In the same manner, β and j_0 are obtained at $C_{H^-} = 1.5 \times 10^{-4}$, 6.0×10^{-4}, and 1.2×10^{-3} mol cm^{-3}, as given in Table 2. The β values are 0.46 ± 0.03 and 0.50 ± 0.01 at $C_{H^-} = 1.5 \times 10^{-4}$ and 3.0×10^{-4} mol cm^{-3}, thereby indicating the symmetrical energy barrier in the range $0.10 \le \eta \le 0.25$ V. In contrast, the β values are 0.68 ± 0.02 and 0.70 ± 0.01 at $C_{H^-} = 6.0 \times 10^{-4}$ and 1.2×10^{-3} mol cm^{-3}, indicating the asymmetrical energy barrier. According to the potential energy surface theory of the transition state,[36,37] the C_{H^-} dependence of β may correspond to the weaker bond between the adsorbed hydrogen atoms and the Zn electrode at the larger C_{H^-} values.

The relation between j_0 and C_{H^-} is shown in Figure 7, and the least-squares fit results in

$$\ln j_0 = \ln(0.23) + (0.45)\ln C_{H^-} \qquad (12)$$

The gradient gives $\beta = 0.55 \pm 0.02$ from eq 8, which corresponds to the symmetrical energy barrier at the equilibrium potential for all C_{H^-} values. The discrepancy of β between this value and those obtained by eq 3 for $C_{H^-} = 6.0 \times 10^{-4}$ and 1.2×10^{-3} mol cm^{-3} may be explained by the potential dependence of β, i.e., β increases with an increase in the potential at large C_{H^-} values. This potential dependence conforms with the variation of gradients of the potential energy surfaces of the reactant (H^-−Li^+) and/or product (H_{ad}(M)−Zn) at their intersection region. In general, such an intersection moves in accordance with the shift of the electrode potential. Since the above reasonable β values are obtained in two ways, the assumption that reaction A is rate-determining is valid under the condition of $(1 - \theta)/(1 - \theta_0) \approx 1$ in reference to the theory of the Tafel slopes and reaction orders for the Volmer−Tafel and Volmer−Horiuti (Volmer−Heyrovsky) reactions.[38,39] If $\theta \approx 1$, then the possibility that reaction C is rate-determining cannot be dismissed because its kinetic equation leads to a similar relation as eq 3.[22] However, θ probably does not become nearly unity at Zn, taking into account its weak hydrogen adsorption property represented by the positive large free energy of adsorption.[19] Thus, reaction C is not likely to be rate-determining.

Conclusions

The hydrogen electrode reaction at a Zn electrode is investigated in a molten LiCl−KCl−LiH system at 673 K. The r_{ct} values in the overpotential region 0.10−0.35 V and the H^- concentration region 1.5×10^{-4}−1.2×10^{-3} mol cm^{-3} are evaluated by electrochemical impedance spectroscopy. Then, j_0 and β are obtained from ln r_{ct}−η plots. The lnj_0− C_{H^-} plot independently gives β. The reasonable β values show that the following reaction

$$H^- \rightleftharpoons H_{ad}(M) + e^-$$

is likely to be the rate-determining step. In this study, while the reaction scheme is not determined completely, the rate-determining step is indicated. Impedance plots also indicate the existence of adsorbed hydrogen atoms on the Zn electrode.

Acknowledgment. Grateful acknowledgment is due to Professor Signe Kjelstrup (Department of Physical Chemistry, Norwegian University of Science and Technology, Norway) and Professor Dick Bedeaux (Leiden Institute of Chemistry, Leiden University, The Netherlands) for their interest in our work and valuable discussions.This study was partly supported by the grant for the "Establishment of the Center of Excellence on Sustainable Energy Systems" program from the Japanese Ministry of Education, Culture, Sports, Science and Technology.

References and Notes

(1) Shearer, R. E.; Werner, R. C. *J. Electrochem. Soc.* **1958**, *105*, 693.
(2) Plambeck, J. A.; Elder, J. P.; Laitinen, H. A. *J. Electrochem. Soc.* **1966**, *113*, 931.
(3) Roy, P.; Salamah, S. A.; Maldonado, J.; Narkiewicz, R. S. *AIP Conf. Proc.* **1993**, *271*, 913.
(4) Rodgers, D. N.; Roy, P.; Salamah, S. A. *AIP Conf. Proc.* **1992**, *246*, 1310.
(5) Mays, G. T.; Smith, A. N.; Engel, J. R. *Distribution and Behavior of Tritium in the Coolant-Salt Technology Facility*, *ORNL/TM-5759*; Oak Ridge National Laboratory, Oak Ridge, TN, 1977.
(6) Maroni, V. A.; Wolson, R. D.; Staahl, G. E. *Nucl. Technol.* **1975**, *25*, 83.
(7) Calaway, W. F. *Nucl. Technol.* **1978**, *39*, 63.
(8) Nohira, T.; Ito, Y. *Electrochemistry* **1999**, *67*, 635.
(9) Nohira, T.; Ito, Y. *J. Electrochem. Soc.* **1997**, *144*, 2290.

(10) Nishikiori, T.; Nohira, T.; Ito, Y. *J. Electrochem. Soc.* **2001**, *148*, E38.
(11) Nishikiori, T.; Nohira, T.; Ito, Y. *J. Electrochem. Soc.* **2001**, *148*, E127.
(12) Indig, M. E.; Snyder, R. N. *J. Electrochem. Soc.* **1962**, *109*, 757.
(13) Takenaka, T.; Ito, Y. *Denki Kagaku oyobi Kogyo Butsuri Kagaku* **1991**, *59*, 759.
(14) Nohira, T.; Ito, Y. *J. Electrochem. Soc.* **2002**, *149*, E159.
(15) Ito, H.; Hasegawa, Y. *J. Electrochem. Soc.* **2000**, *147*, 289.
(16) Ito, H.; Hasegawa, Y.; Ito, Y. *J. Electrochem. Soc.* **2001**, *148*, E148.
(17) Ito, H.; Hasegawa, Y.; Ito, Y. *J. Electrochem. Soc.* **2002**, *149*, E273.
(18) Kita, H. In *Encyclopedia of Electrochemistry of the Elements*; Bard, A. J., Ed.; Marcel Dekker: New York, 1976; Vol. IX, Part A, p 413.
(19) Trasatti, S. *J. Electroanal. Chem.* **1972**, *39*, 163.
(20) Jaksic J. M.; Ristic N. M.; Krstajic N. V.; Jaksic M. M. *Int. J. Hydrogen Energy* **1998**, *23*, 1121.
(21) Nakajima, H.; Nohira, T.; Ito, Y. In *Abstracts of the 31st Symposium on Molten Salt Chemistry*, Sendai, Japan, Nov 11−12, 1999; p 51.
(22) Vetter, K. J. *Electrochemical Kinetics: Theoretical and Experimental Aspects*; Academic Press: New York, 1967.
(23) Horiuchi, J.; Keii, T.; Hirota, K. *J. Res. Inst. Catal., Hokkaido Univ.* **1951**, *2*, 1.
(24) Sharma, R. A.; Seefurth, R. N. *J. Electrochem. Soc.* **1976**, *123*, 1763.
(25) Wen, C. J.; Boukamp, B. A.; Huggins, R. A.; Weppner, W. *J. Electrochem. Soc.* **1979**, *126*, 2258.
(26) Amezawa, K.; Osugi, M.; Tomii, Y.; Ito, Y. *Denki Kagaku oyobi Kogyo Butsuri Kagaku* **1993**, *61*, 736.
(27) Matsunaga, M.; Ito, Y.; Yoshizawa, S. *Denki Kagaku oyobi Kogyo Butsuri Kagaku* **1980**, *48*, 634.
(28) Nakajima, H.; Nohira, T.; Ito, Y. *Electrochem. Solid-State Lett.* **2002**, *5*, E17.
(29) Chase, M. W., Jr. *NIST-JANAF Thermochemical Tables*, 4th ed.; American Institute of Physics: College Park, MD, 1998.
(30) Macdonald, J. R. *Impedance Spectroscopy Emphasizing Solid Materials and Systems*; John Wiley & Sons: New York, 1987; Chapter 2.
(31) Armstrong, R. D.; Henderson, M. *J. Electroanal. Chem.* **1972**, *39*, 81.
(32) Harrington, D. A.; Conway, B. E. *Electrochim. Acta* **1987**, *32*, 1703.
(33) Bai, L.; Harrington, D. A.; Conway, B. E. *Electrochim. Acta* **1987**, *32*, 1713.
(34) Jakšic, J.; Vracăr, Lj.; Neophytides, S. G.; Krstajic, N. *J. New Mater. Electrochem. Syst.* **2004**, *7*, 205.
(35) Kisza, A. *J. Electroanal. Chem.* **2002**, *534*, 99.
(36) Lefebvre, M. C. In *Modern Aspects of Electrochemistry*; Conway, B. E., Bockris, J. O.; White, Ralph E., Eds.; Kluwer Academic/Plenum Publishers: New York, 1999; No. 32, Chapter 3.
(37) Bard, A. J.; Faulkner, L. R. *Electrochemical Methods: Fundamentals and Applications*, 2nd ed.; John Wiley & Sons: New York, 2001; Chapter 3.
(38) Delahay, P. *Double Layer and Electrode Kinetics*; Interscience: New York, 1965; Chapter 10.
(39) Conway, B. E. *Theory and Principles of Electrode Processes*; Modern Concepts in Chemistry; The Ronald Press Company: New York, 1965; Chapter 8.